Measuring the Quantum Efficiency of the Optical Emission of Single Radiating Dipoles Using a Scanning Mirror

B. C. Buchler,[1] T. Kalkbrenner,[1,*] C. Hettich,[1,†] and V. Sandoghdar[1,‡]

[1]*Laboratory of Physical Chemistry, Swiss Federal Institute of Technology (ETH), 8093 Zurich, Switzerland*

(Received 20 January 2005; published 3 August 2005)

Using scanning probe techniques, we show the controlled manipulation of the radiation from single dipoles. In one experiment we study the modification of the fluorescence lifetime of a single molecular dipole in front of a movable silver mirror. A second experiment demonstrates the changing plasmon spectrum of a gold nanoparticle in front of a dielectric mirror. Comparison of our data with theoretical models allows determination of the quantum efficiency of each radiating dipole.

DOI: 10.1103/PhysRevLett.95.063003 PACS numbers: 33.50.−j, 73.20.Mf, 42.50.−p, 68.37.Uv

The radiation of an oscillating electric dipole is modified when placed in front of a planar interface [1]. Investigations of this system date back to Drexhage [2], who studied the influence of a metallic mirror on the fluorescence lifetime of ensembles of Eu^{3+} ions. By preparing many samples, each with a different spacing between the mirror and the ions, two major effects were observed: (1) the decay rate (Γ) oscillates at large distances due to the retarded interaction of the dipoles with their own reflected fields and (2) Γ is strongly modified very close to the mirror as energy is transferred to the metal [1,2]. Since Drexhage, spontaneous emission from ensembles in thin dielectric layers have been well studied [1]. Various key parameters of the radiating dipoles, such as orientation, distance to the interface, and quantum efficiency are, however, averaged in ensemble measurements.

Because of challenges such as detection sensitivity, photostability, and position control, single emitter experiments have been scarce. Some researchers have nevertheless shown effects of the local dielectric environment by adding an index matching fluid to eliminate an interface [3,4] or by introducing a sharp tip [5,6]. In this work we study the fluorescence lifetime and intensity of a single molecule in front of a movable silver mirror. We also examine the plasmon spectrum of a single gold nanoparticle at various locations in front of a dielectric mirror. These experiments allow us to demonstrate, for the first time, both the far-field modulation and the near-field modification of the total decay rate (Γ) for individual dipoles of known orientation. Since the far-field modulations are only due to changes in the radiative decay rate (Γ_r), the quantum efficiency $\eta = \Gamma_r/\Gamma$ of each dipole can be found.

A model of dipole decay in multilayer structures was first developed by Chance *et al.* [7] and has since been expanded to cover many situations. In particular, Sullivan and Hall [8] present an elegant solution that can easily be adapted to our system. For a single dipole at angle θ with respect to the normal of the layers we find [9]:

$$\Gamma = \Gamma_0[1 - \eta_0 + \eta_0(V\cos^2\theta + H\sin^2\theta)], \qquad (1)$$

where η_0 and Γ_0 are the quantum efficiency and decay rate, respectively, in bulk dielectric. The functions V and H are, respectively, the normalized decay rates of dipoles perpendicular and parallel to the layers [8]. These functions depend on the position of the dipole, as well as the thickness and refractive indices of the various layers.

Our experiments used an inverted microscope combined with a shear-force controlled scanning probe [10]. A schematic of the setup used for the single molecule measurements is shown in Fig. 1(a). Samples of highly photostable terrylene molecules embedded in a thin para-terphenyl

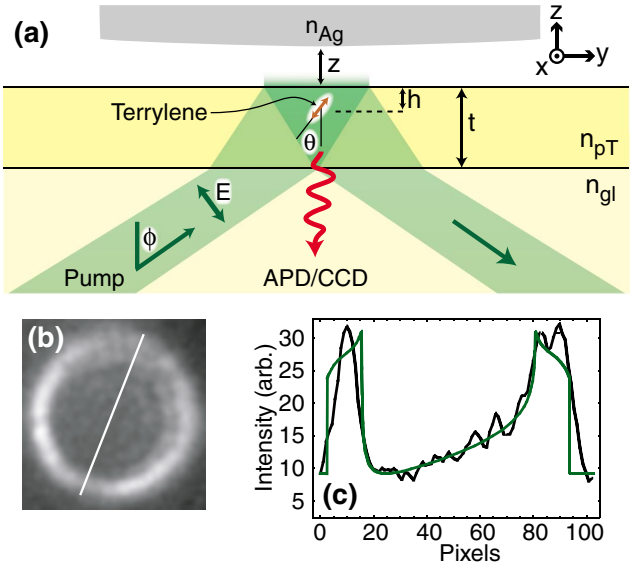

FIG. 1 (color online). (a) Terrylene molecules embedded in para-terphenyl (pT) were illuminated by p-polarized light that undergoes total internal reflection at the pT-air interface. A silver mirror was positioned in front of the sample with a three-dimensional piezo stage (not shown). Fluorescence light is collected and sent to an APD or CCD camera. Parameters used in the modeling are defined in this diagram. (b) The intensity distribution at the back focal plane for a single molecule (with no mirror). (c) A cross section indicated in (b). A fit to this data shows a dipole angle θ of 16° ± 5°.

 © 2005 The American Physical Society

(pT) matrix were prepared following the method described in [11]. The thickness (t) of the pT layer was 35 ± 5 nm as measured using shear-force microscopy. The sample was illuminated by 13 ps pulses of p-polarized 532 nm laser light at a repetition rate of 5 MHz, through an oil immersion objective with a numerical aperture (NA) of 1.4. The laser light was focused in the back focal plane of the objective to give a near-collimated beam at the pT layer. An offset of the beam at the back focal plane resulted in an incidence angle ϕ and total internal reflection at the pT-air interface. The fluorescence of the terrylene ($\lambda \sim 580$ nm) was collected confocally through the objective and sent to an avalanche photodiode (APD) for lifetime measurements or to a CCD for imaging. Above the pT layer, a mirror was mounted in the shear-force stage. The mirror was made by melting an optical fiber tip into a 40 μm diameter ball, which was then coated with 200 nm of silver. As the mirror was lowered onto the pT layer, it reached a point of shear-force "contact" at a height z_0 (typically 5 to 20 nm [10]). The calibrated piezo used in the z axis of the system thus gave an accurate measurement of the mirror-pT distance (z) relative to the zero defined by z_0. With the mirror at z_0, the lateral position of the mirror relative to a molecule could be optimized by maximizing the fluorescence quenching.

Figure 1(b) shows the fluorescence of a single molecule (without the mirror) when it was collected by the objective and sent to the CCD with no further imaging optics. The highly directional (doughnutlike) emission stems from the fact that the terrylene dipole is oriented nearly perpendicular to the substrate plane [11]. As has been shown very recently [12], by analyzing this image we can determine the tilt angle θ of the dipole. From the cross section in Fig. 1(c) we find $\theta = 16^\circ \pm 5^\circ$.

Fluorescence lifetime ($\tau = 1/\Gamma$) was measured via time-correlated single photon counting. Photon arrival times were histogrammed and an exponential decay curve was fitted to find the excited state lifetime. To achieve the required accuracy, 1 to 2 s of data was required per mirror position. In bulk pT the lifetime of terrylene is $\tau_0 = 1/\Gamma_0 = 4.1 \pm 0.1$ ns [13]. In our system (without the mirror) lifetimes were in the range 15 to 25 ns. Increased lifetime is expected for molecules embedded in thin dielectric films [14]. This effect can be described using Eq. (1) and, due to the dependencies of V and H, is highly sensitive to the dipole orientation and depth of each molecule in the film. A particular virtue of single emitter studies is their ability to deal with such inhomogeneities.

We now turn to the lifetime measurements of single molecules as a function of the mirror position z. In total, data were collected from around 15 different molecules. Shown in Fig. 2 are two of these measurements. The lifetime was monitored as the mirror moved towards and away from the molecule, thereby verifying the mechanical stability of the system. We note that more than 5×10^7 photons were detected per molecule, emphasizing the advantage of very high emitter photostability [11].

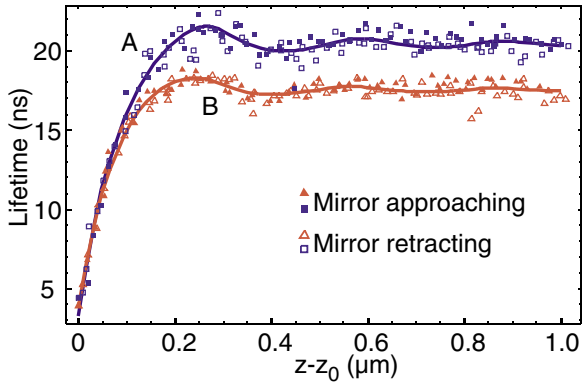

FIG. 2 (color online). Lifetime as a function of mirror position (z) for 2 molecules A (squares) and B (triangles). The solid curves display theoretical fits assuming $\eta_0 = 0.98$, $h = 3$ nm, and $z_0 = 12$ nm for molecule A, $\eta_0 = 1$, $h = 22$ nm, and $z_0 = 11$ nm for molecule B, and $\theta = 16^\circ$ in both molecules.

Figure 2 clearly shows the near-field shortening of the lifetime due to quenching by the metal as well as far-field oscillations that can be understood as being due to the retarded interaction of the dipole with its mirror image [1,2]. The solid curves in the figure show fits to the data made using Eq. (1). The refractive indices n_{gl} and n_{Ag} of glass and silver at 580 nm are taken to be 1.52 and $0.26 + 4i$, respectively. Para-terphenyl is biaxial with refractive indices $n_z = 2.0$, $n_y = 1.69$, and $n_x = 1.59$ [11,15]. In the calculations we take the out-of-plane polarizations to have an index of $(n_x + n_y)/2 = 1.64$. For polarizations parallel to the plane of incidence we assume an index of 1.85 [16]. Using these assumptions, the unknown parameters η_0, h, and z_0 can be approximated by fitting the model to the data. For molecule A we find $0 < h < 13$ nm, $0.9 < \eta_0 < 1$, and $z_0 = 12 \pm 2$ nm whereas for B, $12 < h < 32$ nm, $0.9 < \eta_0 < 1$, and $z_0 = 11 \pm 5$ nm. These values are consistent with what we know about our system. Molecules with longer lifetimes are expected to have smaller depth (h) and the offset (z_0) agrees well with the typical shear-force interaction range of $z_0 < 20$ nm. The estimates of η_0 and h are limited by the uncertainty in the dipole orientation θ, a parameter that is averaged in the theoretical treatments of ensembles, but plays a central role in single emitter studies [4].

The APD also recorded the fluorescence intensity. For molecule B of Fig. 2 this is shown in Fig. 3(a) along with the lifetime data [Fig. 3(b)]. For large z, there is a clear correlation between the intensity and lifetime. The strong intensity modulation is due to our detection optics only seeing a part of the emission pattern while the angular distribution of the fluorescence is changing with the mirror position. The modification of emission patterns due to planar boundaries was originally described by Drexhage [2] and more recently exploited for semiconductor cavity

design [17]. The fluorescence intensity was modeled by finding the emission pattern and then integrating over the numerical aperture of the collection optics [18,19]. Figure 3(c) shows that we must also consider the change in pump intensity experienced by the molecule when the mirror enters the evanescent field above the pT surface. As our measurements were made well below pump saturation, we just multiply the integrated emission pattern by the pump intensity. The solid curve in Fig. 3(a) shows the theoretical fit to the intensity data, displaying reasonable agreement. We note that although the numerical aperture of our objective was 1.4, the intensity modulation is best reproduced by NA = 1. Several factors, such as misalignment of the detection optics or the birefringence of the pT film, could lead to a reduction of the effective numerical aperture. We believe that the main cause of the discrepancy is that the integration of the emission pattern over the numerical aperture assumes the entire dipole-mirror system is at the focus of the objective. This is not actually the case for $z > 500$ nm, equivalent to the Rayleigh range of the microscope objective. In this regime, our high NA confocal detection system begins to lose some of the photons that are first emitted upward and then reflected by the mirror.

We will now consider the second experimental system, namely, a gold nanoparticle in front of a glass substrate. Gold particles can support plasmon resonances that stem from the collective oscillation of electrons in the metal [20]. The plasmon spectrum depends on the size and shape of the particle, as well as the complex dielectric constants of the particle and surrounding medium. In general, the scattering and absorption properties of a nanoparticle can be described by a multipole expansion. For gold particles smaller than about 100 nm, it suffices to consider only dipolar oscillations if one accounts for radiation damping [21]. A small ellipsoidal particle can support 3 independent plasmon dipole modes, one for each axis of the particle [20]. In [22] we describe how a single nanoparticle can be attached to the end of an optical fiber tip. Using such a tip, we then demonstrated a tomographic method to find orientation of the particle axes in the laboratory frame [23]. Here we exploit these techniques to characterize an ellipsoidal nanoparticle (nominal diameter 80 nm) attached to a fiber tip and then monitor the width of one of its plasmon resonances as we move the particle relative to a glass substrate.

Details of the setup and the spectroscopy procedure are given in [23]. In short, the system was illuminated at grazing incidence with white light from a xenon lamp [see Fig. 4(c)]. The scattered light was collected by a microscope objective (NA = 0.85) through the glass substrate and sent to a spectrometer. By performing a tomographic measurement as described in [23], we determined the long axis of the particle to be oriented at $\theta = 10° \pm 2°$. We then rotated the tip about its axis as well as the polarization of the illumination to excite only the long axis plasmon. Figure 4(b) shows the measured plasmon spectrum and a fit obtained using the dipole term of Mie theory with a radiation damping correction [23].

A scanning piezo stage was used to control the distance (z) between the gold particle and a microscope coverglass ($n_{gl} = 1.52$). The point of closest approach (z_0) was defined, as before, by the shear-force interaction. The plasmon decay time was found according to $\tau = 1/(2\pi\gamma)$ [24], where γ (in Hz) is the full-width at half-maximum of the resonance. A plot of the plasmon lifetime and linewidth as a function of z is shown in Fig. 4(a). This result qualitatively resembles that of the molecular dipole. In particular, for large z we see slowly dying oscillations of the lifetime that eventually relax to a value of 2.43 fs. As shown by the solid curve in Fig. 4(a), the data are well reproduced by a theoretical fit according to Eq. (1) [25]. Fitted parameters

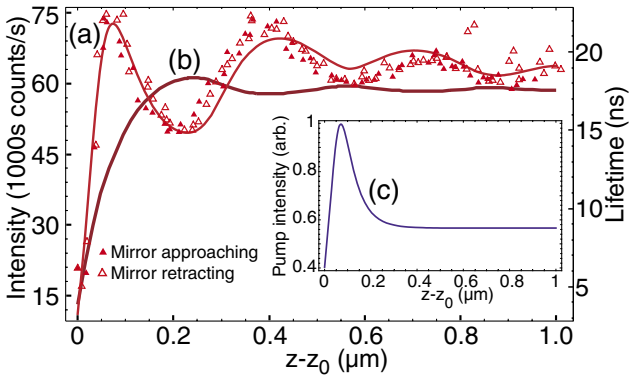

FIG. 3 (color online). (a) (Left-hand axis): symbols show measured intensity of molecule B in Fig. 2. The curve is the theoretical fit to the data with fitted parameters of $\phi = 53 \pm 1$, $NA = 1.00 \pm 0.01$, and other variables as in Fig. 2. (b) (Right-hand axis): the curve B of Fig. 2. (c) The pump intensity at the position of the molecule with $\phi = 53°$.

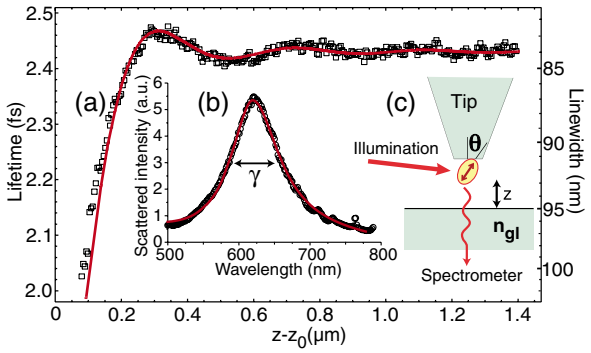

FIG. 4 (color online). (a) The squares show the measured decay time and linewidth of the plasmon oscillations. The solid line shows a theoretical fit using Eq. (1). A stretch factor of 0.8 was fitted to the z axis as the piezo in this system was not calibrated. (b) Circles show a plasmon spectrum recorded from the nanoparticle at the tip. The solid curve is a fit according to a modified Mie theory. (c) A schematic of the setup.

in this case were $z_0 = 9 \pm 6$ nm and $\eta_0 = 0.64 \pm 0.07$. There are two complications in these data that are unique to the gold plasmon measurements. First, the agreement between theory and experiment deteriorates for $z < 200$ nm. We believe that this is because a gold particle close to the glass surface can be no longer treated as a point dipole. Data with $z < 250$ nm are therefore excluded from the fit. Second, the linewidth measurement is affected by interference between the plasmon scattering and stray excitation light [26] that causes a small but constant modulation of the linewidth at large z. This artifact, with peak-to-peak amplitude 0.007 fs and period equal to half the plasmon center wavelength, has been subtracted from the data.

The ''quantum efficiency'' for a classical antenna, such as a gold particle, can again be defined as $\eta = \frac{\Gamma_r}{\Gamma}$. In this case Γ_r and Γ denote the scattering (radiation) and total plasmon relaxation rates, respectively [24,27]. Equivalently, this quantity can be written as $\eta = \frac{\sigma_s}{\sigma_s + \sigma_a}$, where σ_s and σ_a denote the scattering and absorption cross sections of the particle, respectively. Using the outcome of the tomographic measurements and the specified particle size, we calculated the values of σ_s and σ_a according to Mie theory and obtained $\eta_0 = 0.69 \pm 0.07$. Considering the substantial uncertainty in the parameters that enter into the Mie calculation, the agreement between the calculated quantum efficiency and that extracted from the experiment is very good.

In summary, we have demonstrated the *in situ* modification of the decay rate for a single quantum emitter as well as a classical nanoantenna. In both cases the manipulation of a movable external mirror at large distances modifies the dipole's radiative decay rate but leaves its nonradiative dissipation channels unaffected. This enables us to extract the quantum efficiency of a single dipole, a quantity that is nontrivial to determine even for ensembles [28]. Our approach could be extended to various emitters of current interest, ranging from dye molecules and semiconductor nanoparticles to nanotubes. Such measurements would allow the investigation of fluctuations due to variations in the structure of the emitter or its local environment.

We thank A. F. Koenderink and S. Kühn for assistance and fruitful discussions. This work was supported by the Swiss National Science Foundation.

*Present address: FOM Institute for Atomic and Molecular Physics, Kruislaan 407, 1098 SJ Amsterdam, The Netherlands.
†Present address: Niels Bohr Institute, 2100 Copenhagen, Denmark.
‡Electronic address: vahid.sandoghdar@ethz.ch

[1] W. L. Barnes, J. Mod. Opt. **45**, 661 (1998).
[2] K. H. Drexhage, Prog. Opt. **12**, 165 (1974).
[3] J. Macklin, J. Trautman, T. Harris, and L. Brus, Science **272**, 255 (1996).
[4] X. Brokmann, L. Coolen, M. Dahan, and J. P. Hermier, Phys. Rev. Lett. **93**, 107403 (2004).
[5] W. P. Ambrose, P. M. Goodwin, J. C. Martin, and R. A. Keller, Science **265**, 364 (1994).
[6] W. Trabesinger *et al.*, Appl. Phys. Lett. **81**, 2118 (2002).
[7] R. R. Chance, A. Prock, and R. Silbey, Adv. Chem. Phys. **37**, 1 (1978).
[8] K. G. Sullivan and D. G. Hall, J. Opt. Soc. Am. B **14**, 1149 (1997).
[9] L. Novotny, J. Opt. Soc. Am. A **14**, 91 (1997).
[10] K. Karrai and I. Tiemann, Phys. Rev. B **62**, 13174 (2000).
[11] R. J. Pfab *et al.*, Chem. Phys. Lett. **387**, 490 (2004).
[12] M. A. Lieb, J. M. Zavislan, and L. Novotny, J. Opt. Soc. Am. B **21**, 1210 (2004).
[13] G. S. Harms *et al.*, Chem. Phys. Lett. **313**, 533 (1999).
[14] M. Kreiter, M. Prummer, B. Hecht, and U. P. Wild, J. Chem. Phys. **117**, 9430 (2002).
[15] K. Sundararajan, Z. Kristallogr., Kristallgeom., Kristallphys., Kristallchem. **93**, 238 (1936).
[16] The choice of n is not so critical. The model fits our data well for $1.78 < n < 1.95$ and in all cases the value of η is greater than 0.90. The value of 1.85 was found by considering the fraction of power radiated parallel and perpendicular to the slow axis. Previous work has also successfully employed an average index [2,29]. Biaxial layers could, in principle, be included in the model. To our knowledge this has never been done.
[17] H. Benisty, H. DeNeve, and C. Weisbuch, IEEE J. Quantum Electron. **34**, 1612 (1998).
[18] H. Benisty, R. Stanley, and M. Mayer, J. Opt. Soc. Am. A **15**, 1192 (1998).
[19] J. Enderlein, Chem. Phys. **247**, 1 (1999).
[20] U. Kreibig and M. Vollmer, *Optical Properties of Metal Clusters* (Springer, New York, 1995).
[21] A. Wokaun, J. P. Gordon, and P. F. Liao, Phys. Rev. Lett. **48**, 957 (1982).
[22] T. Kalkbrenner, M. Ramstein, J. Mlynek, and V. Sandoghdar, J. Microsc. **202**, 72 (2001).
[23] T. Kalkbrenner, U. Hakanson, and V. Sandoghdar, Nano Lett. **4**, 2309 (2004).
[24] C. Sönnichsen *et al.*, Phys. Rev. Lett. **88**, 077402 (2002).
[25] The fiber tip has a negligible influence on the plasmon spectrum [23]. Moreover, we are only sensitive to *changes* of the plasmon due to the glass substrate while any influence of the tip is constant during the experiment.
[26] T. Kalkbrenner *et al.* (to be published).
[27] E. J. Heilweil and R. M. Hochstrasser, J. Chem. Phys. **82**, 4762 (1985).
[28] G. A. Crosby and J. N. Demas, J. Phys. Chem. **75**, 991 (1971).
[29] R. M. Amos and W. L. Barnes, Phys. Rev. B **55**, 7249 (1997).